

# An inverse cascade model for self-organized complexity and natural hazards

Gleb Yakovlev,<sup>1</sup> William I. Newman,<sup>2</sup> Donald L. Turcotte<sup>3</sup> and Andrei Gabrielov<sup>4</sup>

<sup>1</sup>Computational Science and Engineering Center, University of California, Davis, CA 95616, USA

<sup>2</sup>Departments of Earth and Space Sciences, Physics and Astronomy, and Mathematics, University of California, Los Angeles, CA 90095, USA.

E-mail: win@ucla.edu

<sup>3</sup>Department of Geology, University of California, Davis, CA 95616, USA

<sup>4</sup>Departments of Mathematics and Earth and Atmospheric Sciences, Purdue University, West Lafayette, IN 47907, USA

Accepted 2005 June 22. Received 2005 March 1; in original form 2004 June 12

## SUMMARY

The concept of self-organized complexity evolved from the scaling behaviour of several cellular automata models, examples include the sandpile, slider-block and forest-fire models. Each of these systems has a large number of degrees of freedom and shows a power-law frequency-area distribution of avalanches with  $N \propto A^{-\alpha}$  and  $\alpha \approx 1$ . Actual landslides, earthquakes and forest fires exhibit a similar behaviour. This behaviour can be attributed to an inverse cascade of metastable regions. The metastable regions grow by coalescence which is self-similar and gives power-law scaling. Avalanches sample the distribution of smaller clusters and, at the same time, remove the largest clusters. In this paper we build on earlier work (Gabrielov *et al.*) and show that the coalescence of clusters in the inverse cascade is identical to the formation of fractal drainage networks. This is shown analytically and demonstrated using simulations of the forest-fire model.

**Key words:** complexity, forest-fire model, inverse cascade, power-law scaling, self-organized criticality, Tokunaga network.

## 1 INTRODUCTION

A number of phenomena in geophysics exhibit power-law frequency-magnitude scaling. Earthquakes are a striking example. The rate at which earthquakes occur in a region generally satisfies the Gutenberg & Richter (1954) frequency-magnitude relation

$$\log N_{CE} = -bM + a, \quad (1)$$

where  $N_{CE}$  is the cumulative number of earthquakes with magnitudes greater than or equal to  $M$  in a specified area and time interval. The constant  $b$  or ‘ $b$ -value’ varies from region to region but is generally in the range  $0.8 < b < 1.2$ . The constant  $a$  is a measure of the regional level of seismicity. Aki (1981) has shown that eq. (1) is equivalent to the power-law relation

$$N_{CE} = CA_E^{-(\alpha-1)}, \quad (2)$$

with  $C$  a constant,  $A_E$  the earthquake rupture area and  $\alpha - 1 = b$  in eq. (1). We observe that the negative power-law exponent associated with cumulative distributions is increased by one over the associated probability distribution, since the cumulative distribution function is the integral over the probability distribution. The equivalent non-cumulative frequency-area distribution to eq. (2) has a power-law exponent  $1.8 < \alpha < 2.2$  for the non-cumulative frequency-area statistics of earthquakes.

Large landslides also appear to satisfy power-law frequency-magnitude scaling under a wide variety of conditions (Hovius *et al.* 1997, 2000; Pelletier *et al.* 1997; Guzzetti *et al.* 2002; Malamud *et al.* 2004). This behaviour is observed despite large differences in landslide types, sizes, distributions, patterns and triggering mechanisms. The non-cumulative distribution of large landslides typically satisfies the relation

$$\frac{\delta N_{LS}}{\delta A_{LS}} = CA_{LS}^{-\alpha}, \quad (3)$$

where  $\delta N_{LS}$  is the number of landslides with areas between  $A_{LS}$  and  $A_{LS} + \delta A_{LS}$  and the exponent  $\alpha$  has a value  $\alpha \approx 2.4$ .

The frequency-area distributions of forest and wildfires also are well approximated by a power-law frequency-magnitude relation (Minnich & Chou 1997; Malamud *et al.* 1998; Ricotta *et al.* 1999). The typical exponent for a non-cumulative power-law distribution is  $\alpha \approx 1.4$ . Although forest fires are not strictly geophysical phenomena, they are emphasized in our analysis because they clearly illustrate the role of clustering, which will be the principal focus of this paper.

The concept of self-organized criticality (SOC) was introduced by Bak *et al.* (1988) as a possible explanation for the behaviour of the sandpile model. In this model there is a square grid of boxes and at each time step a particle is dropped into a randomly selected box. When a box accumulates four particles, they are

redistributed to the 4 adjacent boxes, or in the case of edge boxes, lost from the grid. Redistributions can lead to further instabilities, with avalanches of particles lost from the edges of the grid. Because of this avalanche behaviour, this system was given the name ‘sandpile model’. This system, and others like it, manifest ‘avalanches’ with a power-law frequency-size distribution and contains a steady-state ‘input’ with the ‘output’ occurring in the ‘avalanches’. The non-cumulative frequency-area distribution of model avalanches was found to satisfy the power-law distribution

$$N \propto A^{-\alpha}, \quad (4)$$

where  $N$  is the number of avalanches with area  $A$  and  $\alpha$  is a constant with values  $1.0 < \alpha < 1.3$ .

It is natural to associate the sandpile model with naturally occurring landslides. In both cases ‘avalanches’ are associated with metastable regions. For model landslides, the metastable region is the region over which an avalanche spreads when triggered by the addition of a fourth particle in a randomly selected box. Redistributions lead to a sequence of instabilities in boxes. The total number of boxes involved in this sequence of instabilities constitutes the metastable region as well as the avalanche. For actual landslides the metastable region is the region over which the landslide spreads once triggered. For landslides, typical triggering mechanisms are earthquakes, snow-melt events, and severe storms. The fact that the frequency-area distributions of landslides triggered by such events are power law is direct evidence that the distribution of metastable regions is also a power law. It should be noted that the power-law exponent for the model avalanches in a sandpile model is  $\alpha \approx 1.4$ , whereas the exponent for actual landslides is  $\alpha \approx 2.4$ . This difference can be attributed to the 2-D nature of the model versus the 3-D nature of real landslides, since real landslides have a depth as well as an area.

A second model that can exhibit self-organized complexity behaviour is the slider-block model (Carlson & Langer 1989). In this model, an array of slider blocks is connected to a constant velocity driver plate by puller springs and to each other by connector springs. The blocks exhibit stick-slip behaviour due to frictional interactions with the plate across which they are pulled. The frequency-area distribution of the smaller slip events again satisfies eq. (4) with  $1.0 < \alpha < 1.5$  (Carlson & Langer 1989). The area  $A$  is defined to be the number of blocks that participate in a slip event. This model is deterministic, whereas the sandpile model is stochastic.

The relevance of multiple slider-block models to earthquakes was considered (Burrige & Knopoff 1967; Rundle & Jackson 1977) long before the concept of SOC was proposed and the association of SOC behaviour with earthquakes by Bak & Tang (1989). Again, however, the exponents of the power-law behaviour differ. The non-cumulative power-law dependence for earthquakes is  $\alpha \approx 2$ , considerably larger than the value  $1.0 < \alpha < 1.5$  found in slider-block models.

A third model that exhibits SOC is the forest-fire model (Bak *et al.* 1992; Drossel & Schwabl 1992a,b). In the simplest version of this model, a square grid of  $N$  sites is considered. At each time step either a tree is dropped on a randomly chosen site (if the site is unoccupied) or a spark is dropped on the site. The sparking frequency  $f$  is the inverse number of attempted tree drops before a match is dropped. If  $f = 1/100$ , there have been 99 attempts to drop trees (some successful, some unsuccessful) before a spark is dropped at the 100th time step. If the spark is dropped on an empty site, nothing happens. If the spark is dropped on a tree, that tree and all adjacent trees are ‘burned’ in a model ‘forest fire’. The frequency-area distribution of the smaller fires satisfy eq. (4) with  $1.0 < \alpha < 1.3$ . The role of

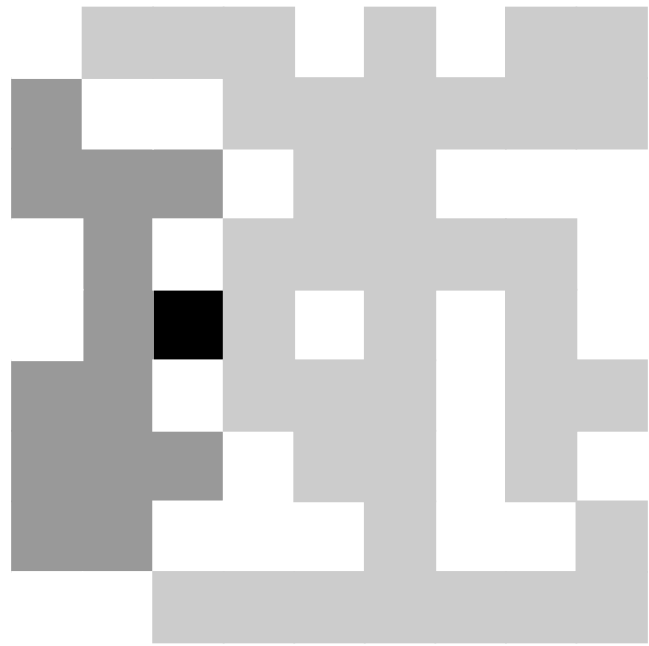


**Figure 1.** The black tree bridges the gap between two clusters, resulting in their coalescence.

metastable regions is clearly illustrated by the forest-fire model. A metastable region is a cluster of adjacent trees that will burn when any one of the trees is ignited by a match. Because the probability of a match landing on a tree cluster is proportional to the area of the cluster  $A_c$  it follows that the number of fires  $N_f$  with area  $A_c$  is related to the number of clusters  $N_c$  with area  $A_c$  by the relation

$$N_f \propto A_c N_c. \quad (5)$$

Since the frequency-area distribution satisfies eq. (4), that is  $N_f \propto A_c^{-\alpha}$ , it follows that

$$N_c \propto A_c^{-\alpha-1}. \quad (6)$$

Tree clusters grow by coalescence. When a newly planted tree bridges the gap between two clusters with  $A_j$  and  $A_i$  trees a new cluster is formed with  $A_i + A_j + 1$  trees, as illustrated in Fig. 1. Trees cascade from smaller to larger clusters until they are lost in the fires that destroy the largest clusters and terminate the cascade. We term this an inverse cascade since the flow of trees is from smaller to larger clusters. Turcotte *et al.* (1999) and Turcotte (1999) quantified this inverse cascade by introducing a collision cross-section for cluster coalescence. They obtained a self-similar cascade that led directly to the applicable equations eqs (4) and (6), for the forest-fire model.

Since these three models have large numbers of degrees of freedom and their behaviour is sensitive to their initial conditions, they are termed ‘complex’. The use of the word ‘criticality’ to describe the behaviour of these models has led to considerable controversy. The formal definition of critical phenomena was introduced by physicists concerned with Hamiltonian systems where the temperature plays a central role in the calculation of the partition function in statistical mechanics—from which all thermodynamic quantities can be calculated—a feature that is absent from the formulation of the class of problems that we wish to address. Also, defining a critical point requires the ‘tuning’ of a control parameter. As discussed above, the forest-fire model has two parameters, the sparking frequency  $f$  and the size of the grid  $N$ . For a specified grid size  $N$ , the sparking frequency  $f$  can be ‘tuned’ so that the largest

fires correspond to the grid size. If the firing frequency is higher, the largest fires will be smaller than the grid size. If the firing frequency is lower, then there will be an excess number of large fires. Grassberger (2002) has recently discussed the details of this ‘criticality’.

However, in all three cases, the frequency-area distribution of fires is a power law satisfying eq. (4). It is this behaviour which we will consider in this paper. Gabrielov *et al.* (1999) have shown analytically that the behaviour of the forest-fire model is the asymptotic outcome of the evolution of a hierarchical set of ordinary differential equations. The behaviour is that of an inverse cascade of clusters of trees. Small clusters coalesce to form larger clusters, and so on. Fires terminate the power-law behaviour of the cascade tuning parameter. Accordingly, what has come to be called SOC by some, we will call without prejudice ‘self-organized complexity’ to avoid any conflict with physicists’ use of these words. Gabrielov *et al.* (1999) further quantified the inverse clustering cascade by introducing cluster orders in direct analogy with the so-called ‘branch orders’ employed to river networks. In this paper we expand on this approach and make direct comparisons with extensive numerical simulations.

## 2 BRANCHING STATISTICS

Long before the concept of either fractals or SOC was introduced, a self-similar stream-ordering system was introduced by Horton (1945) and Strahler (1957). In this classification system, a stream with no upstream tributaries is defined to be of order 1, when two order 1 streams combine, they form a stream of order 2, and so forth. However, when streams of different order combine, the order of the dominant stream prevails. The stream branching networks can be quantified in terms of bifurcation and area-order ratios. The bifurcation ratio  $R_B$  is defined according to

$$R_B = \frac{N_i}{N_{i+1}}, \quad (7)$$

where  $N_i$  is the number of streams of order  $i$  for  $i = 1, 2, \dots$ . The area-order ratio  $R_A$  is defined by

$$R_A = \frac{A_{i+1}}{A_i}, \quad (8)$$

where  $A_i$  is the mean drainage area of all streams of order  $i$ .

Many studies have shown that both  $R_B$  and  $R_A$  are nearly constant for a range of stream orders in any given river network. Pelletier (1999) gives  $R_B \approx 4.26$  and  $R_A \approx 4.6$ . A fractal dimension  $D$  for a river network can be defined according to

$$D = 2 \frac{\ln R_B}{\ln R_A}, \quad (9)$$

with the values for  $R_B$  and  $R_A$  given above for drainage network we have  $D = 1.82$ . Thus drainage networks are slightly less than space filling in two dimensions. River networks were one of the first examples of fractals in nature given by Mandelbrot (1982). A major step forward in classifying river networks was made by Tokunaga (1978). He extended the Strahler (1957) ordering system to include side branching. A first-order branch joining another first-order branch is denoted by the subscript ‘11’ and the number of such branches is  $N_{11}$ ; a first-order branch joining a second-order branch is denoted by the subscript ‘12’ and the number of such branches is  $N_{12}$ ; a second-order branch joining a second-order branch is denoted by the subscript ‘22’ and the number of such branches is  $N_{22}$ . The branch numbers  $N_{ij}$  for a network of order  $n$  constitute a triangular

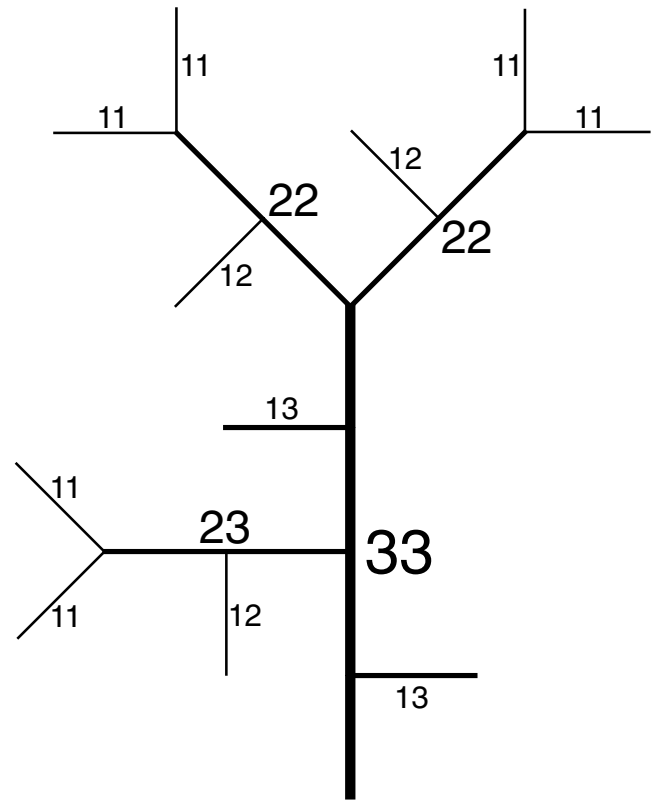


Figure 2. Deterministic third-order Tokunaga network.

matrix. The total number of streams of order  $i$ ,  $N_i$ , is given by

$$N_i = \sum_{j=1}^n N_{ij}. \quad (10)$$

It is convenient to introduce the branching ratio defined by

$$T_{ij} = \frac{N_{ij}}{N_i}. \quad (11)$$

The branching ratio is the average number of branches of order  $i$  joining a branch of order  $j$ . Tokunaga (1978) introduced a required scaling relation for self-similarity

$$T_{i,i+k} = T_k = ac^{k-1}, \quad (12)$$

independent of  $i$ . An example of a deterministic third-order Tokunaga network is shown in Fig. 2. For this example we have:  $N_{11} = 6$ ,  $N_{12} = 3$ ,  $N_{13} = 2$ ,  $N_{21} = 11$ ,  $N_{22} = 2$ ,  $N_{23} = 1$ ,  $N_{31} = 3$ ,  $N_{32} = 1$ ,  $N_{33} = 1$ ,  $T_{12} = T_{23} = T_{11} = 1$ ,  $T_{13} = T_{22} = 2$ . A number of authors (Peckham 1995; Pelletier 1999) have shown that actual drainage networks satisfy this condition with  $c \approx 2.5$  and  $a \approx 1.2$ . A network that satisfies eq. (12) is said to be a Tokunaga network.

Diffusion limited aggregation (DLA) is a simple model that generates a dendritic branching network (Witten & Sander 1981; Turcotte 1997). This model has been applied to a variety of dendritic growth patterns in igneous rocks and other minerals (Fowler 1990). Ossadnik (1992) has shown that DLA networks satisfy the Tokunaga condition eq. (12) with  $a \approx 1.5$  and  $c \approx 2.7$ .

We now apply the concepts of self-similar branching to the self-similar coalescence of clusters. Our approach is based on a modified version of the forest-fire model. Trees are randomly planted on a square grid. Clusters are allowed to grow by coalescence until they reach a specified size. When a cluster of trees reaches this specified size it is removed (burned). One version of this model was studied

by Newman & Turcotte (2002). Clusters were removed when they spanned the grid (percolated). The reason for using this modified version of the forest-fire model is to extend the scaling region to the largest fires. Both models have identical behaviours for smaller clusters and smaller fires.

Our model exhibits a steady-state behaviour. Clusters grow and are lost, but at any point in time there is a number-area distribution of clusters that is only weakly dependent on time. Clusters are continuously coalescing and our object is to associate a cluster order with each cluster on the grid. A cluster on the grid that has not combined with another cluster is a first-order cluster. When two first-order clusters coalesce they form a second-order cluster. When two clusters of order  $i$  coalesce they form a cluster of order  $i + 1$ , that is,

$$N_i \rightarrow N_i - 2, N_{i+1} \rightarrow N_{i+1} + 1. \tag{13}$$

We neglect the rare events when more than two clusters coalesce on a single time step. When a cluster of order  $j$  coalesces with a cluster of order  $i$  there is no change in the number of clusters of order  $j$ , for  $j > i$ , namely,

$$N_i \rightarrow N_i - 1, N_j \rightarrow N_j. \tag{14}$$

In addition to the number of clusters of order  $i$ ,  $N_i$ , we will also consider the mean area  $A_i$  of all clusters of order  $i$ .

In analogy to the side branching statistics of river networks we will consider the similar statistics of cluster coalescence. A first-order cluster coalescing with another first-order branch is denoted by the subscript ‘11’, a first-order cluster coalescing with a second-order cluster is denoted by ‘12’, and an  $i$ th order cluster coalescing with a  $j$ th order cluster is denoted by ‘ $ij$ ’. We will consider orders of all clusters that have coalesced to form each cluster on the grid. When a cluster of order  $i$  joins a cluster of order  $j$ , the history of subclusters in the cluster of order  $i$  is erased. Only the order of the clusters that have actually coalesced to form a higher order cluster are tracked.

### 3 INVERSE CASCADE MODEL

In our inverse cascade model, we assume that each cluster of order  $i$  has an area  $A_i$ . In terms of numerical simulations, this is the mean area of clusters of order  $i$ . We also introduce a rate of coalescence  $r_{ij}$  between clusters of order  $i$  and  $j$ . We assume that this rate is proportional to the number of clusters of order  $i$ , namely  $N_i$ , and the number of clusters of order  $j$ , namely  $N_j$ . We also assume that the rate is proportional to the areas  $A_i$  and  $A_j$  raised to a power  $\beta$ . This scaling is an attempt to represent an ‘effective’ cluster perimeter. [For example, Euclidean clusters would have  $\beta = 0.5$ . See Gabrielov *et al.* (1999) for an earlier approach to this problem.] For near circular clusters, the static ‘cross-section’ for coalescence would be expected to be linearly dependent on the linear dimension of the cluster, i.e.  $\beta \approx 0.5$ . For more dendritic clusters the value of  $\beta$  would be expected to be larger. In addition we introduce a scaling factor  $\epsilon^{-(i-j)}$ , to account for the fractal structure of the clusters. We expect the self-similar cluster coalescence to depend on the difference in orders of the two clusters. On this basis we write

$$r_{ij} = R\epsilon^{-(j-i)}N_iN_jA_i^\beta A_j^\beta, \tag{15}$$

where  $R$  is a constant. We further assume a steady-state behaviour so that  $N_i$  and  $A_i$  are not time dependent. We will discuss this in more detail in the simulation section.

In the spirit of Gabrielov *et al.* (1999), we develop balance equations for the number  $N_i$  and mean area  $A_i$  for the  $i$ th order clusters.

For single tree, order 1 clusters, this balance requires

$$C = 2r_{11} + \sum_{j=2}^{\infty} r_{1j}, \tag{16}$$

where  $C$  is the planting rate of single tree, order 1, clusters. Since we are assuming steady-state behaviour, this gain in clusters must be balanced by the loss of order 1 clusters. The first term on the right represents the loss of two order 1 clusters when they combine to form an order 2 cluster. The summation over orders 2 to  $\infty$  accounts for the coalescence of order 1 clusters with clusters of higher orders.

For clusters of order  $i$  we write

$$r_{i-1,i-1} = 2r_{ii} + \sum_{j=i+1}^{\infty} r_{ij}, \tag{17}$$

where the term on the left is the rate at which clusters of order  $i$  are formed by the coalescence of two clusters of order  $i - 1$ . Note that this is the only way in which a cluster of order  $i$  can be formed. The first term on the right represents the loss of two order  $i$  clusters when they combine to form a cluster of order  $i + 1$ . The summation over orders  $i + 1$  to  $\infty$  accounts for the coalescence of order  $i$  clusters with higher order clusters.

Substitution of the rates of coalescence  $r_{ij}$  from eq. (15) into eqs (16) and (17) gives

$$C = 2RN_1^2 + R \sum_{j=2}^{\infty} \epsilon^{-(j-1)}N_1N_jA_j^\beta, \tag{18}$$

where we note that  $A_1 = 1$  and

$$N_{i-1}^2A_{i-1}^{2\beta} = 2N_i^2A_i^{2\beta} + \sum_{j=i+1}^{\infty} \epsilon^{-(j-i)}N_iN_jA_i^\beta A_j^\beta. \tag{19}$$

We now seek a self-similar solution by assuming that

$$N_iA_i^\beta = N_1x^{i-1}. \tag{20}$$

Substitution of this scaling into eqs (18) and (19) gives

$$C = 2RN_1^2 + RN_1^2 \sum_{j=2}^{\infty} \left(\frac{x}{\epsilon}\right)^{j-1} \tag{21}$$

and

$$x^{2i-4} = 2x^{2i-2} + \frac{x^{2i-1}}{\epsilon} \sum_{j=i+1}^{\infty} \left(\frac{x}{\epsilon}\right)^{j-i-1}. \tag{22}$$

Noting that with  $k = j - i - 1$  we have (sum of the infinite geometrical series)  $\sum_{k=0}^{\infty} (\frac{x}{\epsilon})^k = 1/(1 - x/\epsilon)$  and we can rewrite eqs (21) and (22) as

$$C = RN_1^2 \left(2 + \frac{x}{\epsilon - x}\right) \tag{23}$$

and

$$1 = 2x^2 + \frac{x^3}{\epsilon - x} = x^2 \left(2 + \frac{x}{\epsilon - x}\right). \tag{24}$$

From eq. (24) we obtain an expression for  $\epsilon$  in terms of  $x$ , namely

$$\epsilon = \frac{x - x^3}{1 - 2x^2}. \tag{25}$$

In the Euclidean limit,  $\epsilon = 1$  we have  $x = 0.55496$ . Substitution of eq. (24) into eq. (23) gives

$$N_1 = x\sqrt{C/R}. \tag{26}$$

We next write a steady-state balance equation for the mean cluster areas  $A_i$ . For clusters of order  $i$  we have

$$2r_{i-1,i-1}A_{i-1} + \sum_{k=1}^{i-1} r_{ik}A_k = 2r_{ii}A_i + \sum_{j=i+1}^{\infty} r_{ij}A_i. \tag{27}$$

The first term on the left is the area increase when two clusters of order  $i - 1$  coalesce to form a cluster of order  $i$ . The second term on the left accounts for area increase due to the coalescence of clusters of order 1 to  $i - 1$  with clusters of order  $i$ . The first term on the right represents the loss of area when two clusters of order  $i$  merge to form a cluster of order  $i + 1$ . The second term on the right accounts for loss of area due to the coalescence of clusters of order  $i$  with clusters of orders  $i + 1$  to infinity.

Substitution of the rates of coalescence  $r_{ij}$  from eq. (15) into eq. (27) gives

$$2N_{i-1}^2 A_{i-1}^{1+2\beta} + \sum_{k=1}^{i-1} \epsilon^{-(i-k)} N_i N_k A_i^\beta A_k^{1+\beta} = 2N_i^2 A_i^{1+2\beta} + \sum_{j=i+1}^{\infty} \epsilon^{-(j-i)} N_i N_j A_i^{1+\beta} A_j^\beta. \quad (28)$$

Substitution of the scaling relation eq. (20) into eq. (28) gives

$$2x^{2(i-2)} A_{i-1} + x^{i-1} \sum_{k=1}^{i-1} \epsilon^{-(i-k)} x^{k-1} A_k = 2x^{2(i-1)} A_i + \frac{A_i x^{2i-1}}{\epsilon} \sum_{j=i+1}^{\infty} \left(\frac{x}{\epsilon}\right)^{j-i-1}. \quad (29)$$

Assuming the further self-similar scaling relation

$$x^{i-1} A_i = y^{i-1} \quad (30)$$

and using eq. (24), the sum of the infinite geometrical series, and eq. (30), we find that eq. (29) reduces to

$$2xy^{i-2} + x^2 \epsilon^{1-i} \sum_{k=1}^{i-1} (\epsilon y)^{k-1} = y^{i-1}. \quad (31)$$

The summation in this equation can be simplified using

$$\sum_{k=1}^{i-1} (\epsilon y)^k = \frac{(\epsilon y)^{i-1} - 1}{\epsilon y - 1}. \quad (32)$$

Substitution of eq. (32) into eq. (31) gives

$$2xy^{i-2} + \epsilon^{1-i} x^2 \left[ \frac{(\epsilon y)^{i-1} - 1}{\epsilon y - 1} \right] = y^{i-1}. \quad (33)$$

This equation has a similarity solution only for large values of  $i$ , that is when  $(\epsilon y)^{i-1} \gg 1$ , whereupon in this limit eq. (33) becomes

$$2\frac{x}{y} + \frac{x^2}{\epsilon y - 1} = 1. \quad (34)$$

Comparing eq. (24) with eq. (34), we observe that they become identical if and only if we select

$$y = \frac{1}{x}. \quad (35)$$

Substitution of eq. (35) into eq. (30) gives

$$A_i = x^{-2(i-1)}. \quad (36)$$

From eq. (8) it follows that the area-order ratio  $R_A$  for clustering is given by

$$R_A = \frac{A_{i+1}}{A_i} = \frac{1}{x^2}. \quad (37)$$

The area-order scaling for clusters satisfies the same self-similar scaling as drainage networks. In the Euclidean limit with  $\epsilon = 1$  and  $x = 0.55496$ , we have  $R_A = 3.2823$ .

Substitution of eq. (36) into eq. (20) gives

$$N_i = N_1 x^{(1+2\beta)(i-1)}. \quad (38)$$

From eq. (7) it follows that the bifurcation ratio  $R_B$  for clustering is given by

$$R_B = \frac{N_i}{N_{i+1}} = \frac{1}{x^{1+2\beta}}. \quad (39)$$

The number-order scaling for clusters is also self-similar. In the Euclidean limit  $\beta = 1/2$  and  $\epsilon = 1$  we have  $R_B = R_A = x^{-2}$ . Combining eqs (36) and (38) gives

$$N_i = N_1 A_i^{-\frac{1+2\beta}{2}}. \quad (40)$$

Thus our inverse cascade model gives power-law scaling. It must be noted that our introduction of cluster orders is equivalent to logarithmic binning so that eq. (40) is equivalent to the cumulative distribution given in eq. (2). Thus we have

$$\alpha = \beta + \frac{3}{2}. \quad (41)$$

In the Euclidean limit  $\beta = 1/2$ , we have  $\alpha = 2$ .

It is also of interest to determine the mean lifetime of clusters of order  $i$ ,  $\tau_i$ . In terms of the planting rate of single trees  $C_1$  introduced in eq. (16), the mean lifetime of clusters of order 1 is

$$\tau_1 = \frac{N_1}{C}. \quad (42)$$

Since  $r_{i-1,i-1}$  is the rate of formation of clusters of order  $i$ , the mean lifetime of clusters of order  $i$  is given by

$$\tau_i = \frac{N_i}{r_{i-1,i-1}}. \quad (43)$$

Substitution of  $r_{i-1,i-1}$  from eq. (15) gives

$$\tau_i = \frac{N_i}{RN_{i-1}^2 A_{i-1}^{2\beta}} \quad (44)$$

and further substitution of eqs (20), (38) and (26) gives

$$\tau_i = \frac{N_1}{C} x^{(2\beta-1)(i-1)}. \quad (45)$$

In the Euclidean limit  $\beta = 1/2$  we have  $\tau_i = N_1/C = \tau_1$  and clusters of all orders have the same mean lifetime.

In analogy to the branching ratios for stream networks,  $T_{ij}$  defined in eq. (11), we introduce a cluster coalescence ratio  $T_{ij}$  that is the average number of clusters of order  $i$  that coalesce with a cluster of order  $j$ . In terms of the rate of coalescence between clusters of order  $i$  and  $j$ ,  $r_{ij}$  defined in eq. (15), we can write

$$t_{ij} = \frac{r_{ij} \tau_j}{N_j}. \quad (46)$$

Substitution of eq. (15) gives

$$t_{ij} = R \tau_j \epsilon^{-(j-i)} N_i A_i^\beta A_j^\beta. \quad (47)$$

Further substitution of eqs (20), (36), (45), and (26) reduces this to

$$t_{ij} = x^2 (\epsilon x)^{-(j-i)}. \quad (48)$$

Letting  $k = j - i$  this can also be written as

$$t_{i,i+k} = t_k = \frac{x}{\epsilon} \left(\frac{1}{\epsilon x}\right)^{k-1}. \quad (49)$$

Thus our self-similar cluster coalescence satisfies the Tokunaga self-similar branching statistics introduced in eq. (12) with  $a = x/\epsilon$  and  $c = (\epsilon x)^{-1}$ . In the Euclidean limit with  $\epsilon = 1$  and  $x = 0.55469$ , we have  $a = 0.55469$  and  $c = 1.8028$ .

#### 4 NUMERICAL SIMULATIONS

In order to test the self-similar analysis of cluster coalescence given above, we have carried out a series of numerical simulations. These simulations use a modified version of the forest-fire model as described previously. A square  $L \times L$  grid of sites is considered. A site is chosen at random at each time step, and a tree is planted on the site if it is unoccupied. Cluster sizes of trees grow by coalescence primarily when a planted tree bridges the gap between two adjacent clusters as illustrated in Fig. 2.

The order of each cluster as defined above is tracked and the number of clusters and their areas are determined. Clusters at or above a prescribed area threshold are removed from the grid at the time when they form. This allows us to avoid the space filling implied in our analysis presented above. A particular value of this prescribed threshold is based on percolation theory results (Stauffer & Aharony 1994). It is known that the largest cluster at the percolation threshold is on the verge of becoming a space-filling object. We choose the area threshold to be about 10 times smaller than the area of the percolation cluster at the percolation threshold which scales  $\propto L^{1.895}$  with the linear grid size  $L$ . It should be noted that our numerical results do not change significantly when we vary the area threshold value by an order of magnitude in either direction. After a sufficiently long initial transient, the system experienced only small fluctuations for major system parameters like average grid occupancy and average cluster count. Thus, the model is in a quasi-steady state with a continuous introduction of single trees and the removal of trees when they are in a cluster of the prescribed maximum area. There is an inverse cascade of trees from clusters of lower order to clusters of higher order. The orders of all subclusters that have coalesced to each cluster are tracked.

For the simulation reported here we utilized a  $30\,000 \times 30\,000$  grid. Clusters at and above 2 per cent of the grid size were instantaneously removed from the grid when formed by coalescence. A typical distribution of tree clusters on the grid is given in Fig. 3. The number of clusters of order  $i$ ,  $N_i$ , and the mean area of clusters of order  $i$ ,  $A_i$  are given in Fig. 4.

The mean cluster areas are well represented by the power-law fit

$$A_i = 0.06 \times (4.325)^{i-1}. \quad (50)$$

From eq. (37) this corresponds to an area-order ratio  $R_A = 4.325$  and gives  $x = 0.4808$ . From eq. (25) we find that the required scaling factor is  $\epsilon = 0.6875$ .

From Fig. 4 we also see that cluster numbers  $N_i$  are well fitted by the power-law

$$N_i = 5 \times 10^{10} (0.186)^{i-1}. \quad (51)$$

From eq. (39) this corresponds to a bifurcation ratio  $R_B = 5.376$ . Taking  $x = 0.4808$  from the above, we find from eq. (39) that  $\beta = 0.6484$ . This is somewhat larger than the Euclidean value  $\beta = 0.5$ .

For each cluster order, the number of clusters  $N_i$  is plotted against the mean cluster area  $A_i$  in Fig. 5. This dependence is well represented by the power-law fit

$$N_i = 8 \times 10^9 A_i^{-1.147}. \quad (52)$$

Since the binning by order is equivalent to a cumulative distribution, we find from eq. (2) that  $\alpha = 2.147$ . Also included in Fig. 5 is the actual frequency-area distribution of clusters as measured. The power-law fit for this dependence is given by

$$N_A = 8 \times 10^9 A^{-2.184}. \quad (53)$$

Since this is a non-cumulative distribution we find using eq. (4) that  $\alpha = 2.184$ . The two distributions in Fig. 5 are in quite good agreement.

The dependency of the mean lifetime  $\tau_i$  of clusters of order  $i$  is shown in Fig. 6. For cluster orders 2 to 9 this dependence is well represented by the power-law fit

$$\frac{\tau_i}{\tau_2} = 0.755^{i-2}. \quad (54)$$

Comparing eq. (45) with eq. (54) we require

$$0.775 = x^{2\beta-1}. \quad (55)$$

Taking  $x = 0.4808$  as obtained from eq. (50), we require from eq. (55) that  $\beta = 0.692$ . This compares with the value  $\beta = 0.6484$  obtained previously from eq. (51). These two values are in reasonably good agreement. The results given in Fig. 6 deviate from the power-law correlation for orders 10 to 12. We attribute this deviation to the termination of the cascade so that clusters of these orders are not lost to higher order clusters and their lifetimes are longer than those given by the power-law scaling in eq. (54).

We have also obtained the cluster coalescence ratios  $t_{ij}$ . These values are tabulated in Table 1. Our inverse cascade model predicts that the  $t_{i,i+k}$  should be independent of  $i$ . An inspection of the data in Table 1 shows that this condition is reasonable well approximated. Using the values given in the Table 1 we find the mean value of the  $t_{i,i+k}$  for each  $k$  using

$$t_k = \frac{1}{n-k} \sum_{i=1}^{n-k} t_{i,i+k}, \quad (56)$$

where  $n$  is the total number of orders considered. The resulting values of  $t_k$  are plotted against  $k$  in Fig. 7. This dependence is reasonably well represented by the power-law fit

$$t_k = 2.778^{k-1}. \quad (57)$$

Comparing eq. (49) with eq. (57), we require

$$2.778 = \frac{1}{\epsilon x}. \quad (58)$$

Taking  $x = 0.4808$  as obtained from eq. (50), we require  $\epsilon = 0.749$ . This is about 10 per cent larger than the value obtained previously. In general, we conclude that the agreement between our simulations and predictions of the inverse cascade model are quite good.

#### 5 DISCUSSION

In this paper, we have developed an inverse cascade model for the scale-invariant development of metastable regions. The inverse cascade is dominated by the coalescence of metastable clusters. We have shown that the statistics of coalescence are identical to the statistics of self-similar drainage networks. We have verified the applicability of our model using numerical simulations of a modified form of the forest-fire model.

We will now show that our inverse-cascade model is also applicable to the standard forest-fire model in its scaling region. To do this, we will show that, in the standard model, significant numbers of trees are lost only in the largest model fires. As discussed above, the rate  $r_{fi}$  at which trees in clusters of order  $i$  are burned in model fires is given by

$$r_{fi} \propto A_i N_{fi} \propto A_i^2 N_i, \quad (59)$$

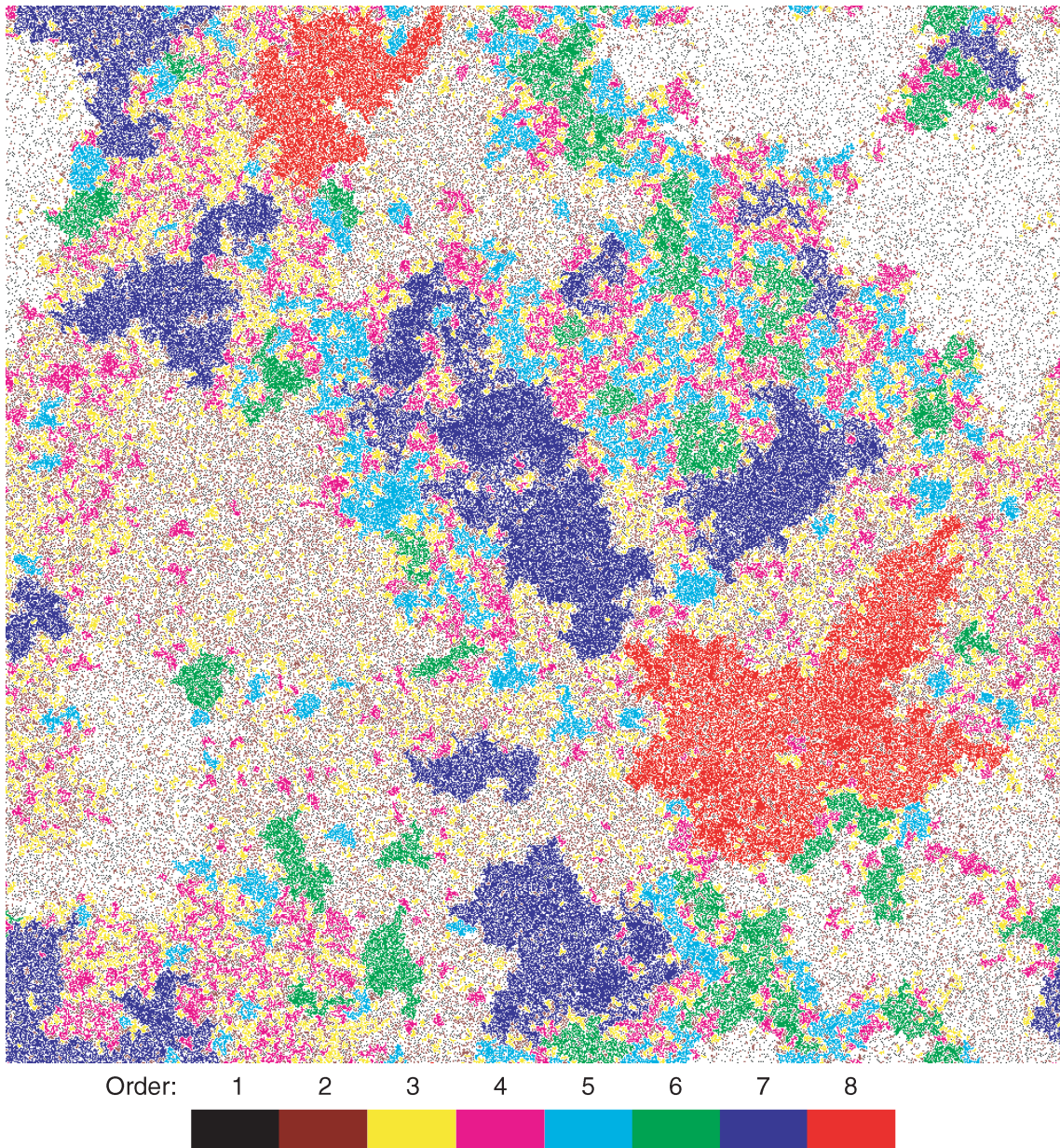


**Figure 3.** A typical distribution of trees on the grid. The clusters of different orders are colour coded.

since  $N_{fi} \propto A_i N_i$ . The rate  $r_{ci}$  at which trees pass through clusters of order  $i$  in our inverse cascade model is given by

$$r_{ci} \propto \frac{A_i N_i}{\tau_i}. \quad (60)$$

Combining eqs (59) and (60) gives

$$\frac{r_{fi}}{r_{ci}} \propto \frac{A_i}{\tau_i}. \quad (61)$$

Substitution of eqs (36) and (45) gives

$$\frac{r_{fi}}{r_{ci}} \propto x^{-(1+2\beta)i}. \quad (62)$$

For our simulations, we found  $x \approx 0.4808$  and  $\beta = 0.6484$ ; substituting these values into eq. (62), we find

$$\frac{r_{fi}}{r_{ci}} \propto 2.08^{2.30i}. \quad (63)$$

Thus,  $r_{fi}/r_{ci} \ll 1$  except for the largest values of  $i$  (largest clusters). Very few trees are burned by fires that destroy the smaller clusters. The role of model fires in eliminating trees is restricted to the highest order  $i$  (largest) clusters. In the forest-fire model, significant numbers of trees are lost only in the highest order (largest) clusters. There is an inverse cascade of trees from the smallest clusters to the largest clusters that terminate the cascade and its power-law region. The firing frequency  $f$  determines the size (order  $i$ ) of the largest clusters but does not effect the scaling region.

The discovery by Bak *et al.* (1988) of the behaviour of the original sandpile model represented a major step in the subject of self-organizing complexity. The steady-state behaviour of the model with a steady input and an output in avalanches with a power-law frequency-size distribution is now recognized as being quite universal. The only variable parameter in this model is the system size. The power-law distribution of avalanches extends to this size. We believe our inverse-cascade model provides a direct explanation for

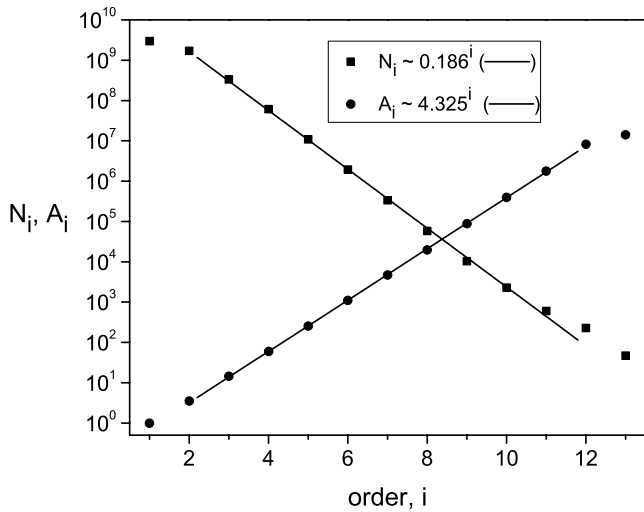


**Figure 4.** Dependence of the number of clusters of order  $i$ ,  $N_i$ , and the mean area of clusters of order  $i$ ,  $A_i$  on cluster order  $i$ . The straight line correlation with the number  $N_i$  is from eq. (51) and the straight line correlation with areas is from eq. (50).

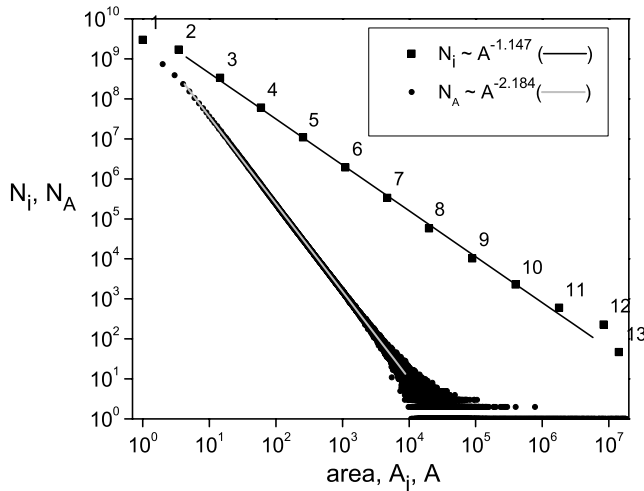


**Figure 5.** The square data points give the dependence of the number of clusters of order  $i$ ,  $N_i$ , on the mean area of clusters of order  $i$ ,  $A_i$ . The straight line is the power-law correlation with eq. (4) taking  $\alpha = 1.147$ . The circular points give the dependence of the number of clusters  $N_A$  of area  $A$  on the area  $A$ . The straight line correlation is with eq. (4) taking  $\alpha = 2.184$ .

the behaviour of this model. The boxes over which an avalanche spreads once triggered corresponds to our metastable clusters. As in our model, the metastable regions grow by coalescence.

A second model that exhibits this behaviour is the slider-block model. The two important parameters are the system size (number of blocks) and the stiffness (the ratio of the connecting spring constant to the driver spring constant). For large system sizes, the size of the largest avalanches (slip events) is determined by the stiffness. The role of the stiffness parameter in the slider-block model is identical to the role of the sparking frequency  $f$  in the forest-fire model. The metastable region is the region over which a slip event spreads when the force on any single block exceeds the static frictional resistance. Once again, we attribute the power-law frequency-area scaling of slip events to the coalescence of metastable regions in an inverse

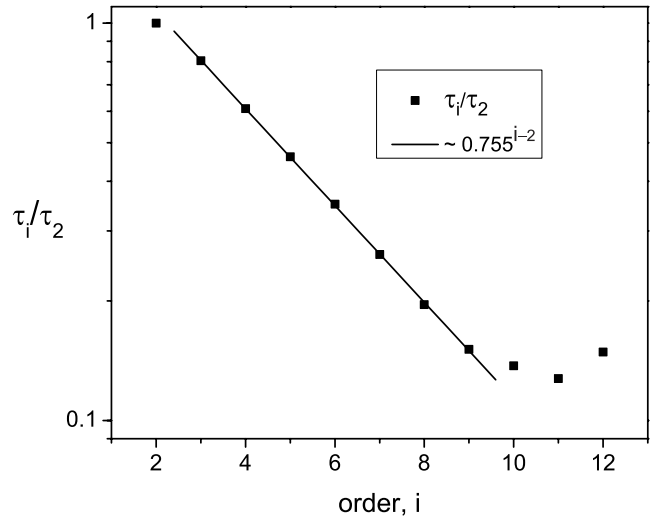


**Figure 6.** Dependence of the mean lifetime of clusters of order  $i$ ,  $\tau_i$ , on order  $i$ . The straight line correlation is with the relation  $\tau_i/\tau_2 = 0.755^{i-2}$ .

cascade. It should be noted that the behaviour of slider-block models can be quite complex (Rundle & Klein 1993).

Ben-Zion *et al.* (2003) pointed out that the evolution of seismicity on a heterogeneous fault in an elastic solid is associated with both direct and inverse cascades. The inverse cascade involves the coalescence of stress fluctuations to larger scales in analogy to the coalescence of tree clusters in this paper. The direct cascade is associated with transfer of stress from large wavenumber scales to short wavenumber scales. The loading of the fault through tectonics is at the largest scale.

The behaviour of the forest-fire model is clearly explained in terms of an inverse cascade. Individual trees are planted and clusters of trees grow by coalescence. The primary mechanism for the coalescence of clusters is bridging of gaps between clusters as illustrated in Fig. 1. The inverse cascade is further quantified by introducing the concept of a cluster order which is identical to the classification of stream networks illustrated in Fig. 2. The joining of streams as stream networks evolve is analogous to the coalescence of clusters as they grow. Streams can be classified according to both the primary branching and side or secondary branching. Clusters can be similarly defined. When two clusters of equal order coalesce it is analogous to the joining of two streams of the same order. When a cluster of lower order coalesces with a cluster of higher order it is analogous to the side branching between a stream of lower and higher order.

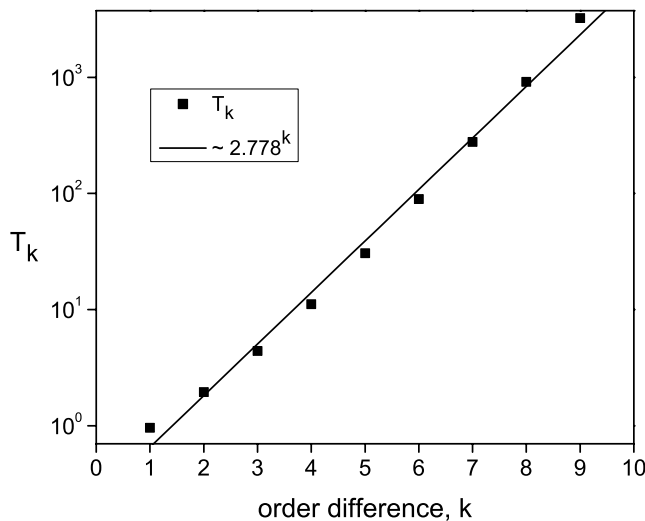
In the forest-fire model, fires sample the population of smaller clusters but do not deplete their number. Individual trees cascade from smaller clusters to larger clusters until the cascade is terminated in the largest fires. These largest fires define the upper limit of the power-law frequency-area scaling of both clusters and fires.

In this paper the behaviour of the cascade is quantified in terms of balance equations for the creation and loss of clusters of each order. The cascade is self-similar and the populations of clusters in terms of primary and secondary coalescences are identical to the populations of branches in Tokunaga self-similar drainage networks. In this paper we have also carried out extensive simulations that confirm the self-similar behaviour given by the cascade model.

The behaviour of the forest-fire model in terms of an inverse-cascade also explains the behaviour of the sandpile and slider-block models. In each case there are metastable regions over which a

**Table 1.** Cluster coalesce ratios  $t_{ij}$  from our simulations.

Order	$i = 2$	3	4	5	6	7	8	9	10
$j = 3$	0.98								
4	1.76	0.95							
5	3.65	1.86	0.96						
6	8.48	3.99	1.91	0.95					
7	20.86	9.26	4.08	1.88	0.94				
8	55.11	23.31	9.69	4.10	1.87	0.93			
9	167.50	67.35	26.55	10.38	4.24	1.90	0.93		
10	634.40	240.70	89.49	32.69	12.10	4.70	2.02	0.96	
11	3243.00	1192.00	425.40	146.60	49.49	16.89	6.06	2.40	1.07

**Figure 7.** Dependence of the mean cluster coalescence ratios  $t_k$  on  $k$ . The straight line is the Tokunaga scaling from eq. (49) with  $(\epsilon x)^{-1} = 2.778$ .

triggered avalanche spreads. In the forest-fire model the metastable regions are the tree clusters. Once ignited, the tree cluster is eliminated by the resulting fire. In the sandpile model the metastable region is the group of boxes over which an avalanche spreads when it is initiated by the addition of a fourth particle to a box. In the slider-block model the metastable region is the group of blocks over which a slip event spreads when any one block begins to slip (when the force on the block exceeds the static friction resisting motion).

The concepts presented in this paper are also applicable to the three natural hazards discussed previously. Despite the many factors influencing forest fires (vegetation, topography, winds, fire-fighting efforts) the frequency-area distributions of actual forest fires are remarkably similar to the behaviour of the forest-fire model. In the case of landslides the metastable regions are the regions over which landslides spread once triggered. Typical landslide triggers are earthquakes, snow-melt events and severe rain storms. The observed power-law frequency-size distribution of large landslides is the evidence that the frequency-area distribution of metastable regions is also power law. These metastable regions grow as a mountain region experiences tectonic uplift. We argue that this growth of metastable regions is dominated by the coalescence of smaller metastable regions.

In the case of earthquakes, the metastable region is the region over which a rupture spreads once triggered. Scaling studies—see for example Turcotte (1997)—have shown that the total offset on faults scales with a power-law dependence on the length of the fault. The increase in fault length is likely to occur by the coalescence of smaller faults to form large faults.

## ACKNOWLEDGMENTS

The authors thank Yehuda Ben-Zion and an anonymous reviewer for useful suggestions for improving this paper. This research has been supported by the National Science Foundation under Grantw ATM-0327558 (WIN), ATM-0327571 (DLT), and ATM-0327598 (AG).

## REFERENCES

- Aki, K., 1981. A probabilistic synthesis of precursory phenomena, in *Earthquake Prediction*, pp. 566–574, eds Simpson, D.W. & Richards, P.G., American Geophysical Union, Washington, DC.
- Bak, P. & Tang, C., 1989. Earthquakes as a self-organized critical phenomenon, *J. geophys. Res.*, **94**, 15 635–15 637.
- Bak, P., Tang, C. & Wiesenfeld, K., 1988. Self-organized criticality, *Phys. Rev. A*, **38**, 364–374.
- Bak, P., Chen, K. & Tang, C., 1992. A forest fire model and some thoughts on turbulence, *Phys. Lett. A*, **14**, 297–300.
- Ben-zion, Y., Eneva, Y. & Liu, Y., 2003. Large earthquake cycles and intermittent criticality on heterogeneous faults due to evolving stress and seismicity, *J. geophys. Res.*, **108**(B6), 2307.
- Burridge, R. & Knopoff, L., 1967. Model and theoretical seismicity, *Bull. seism. Soc. Am.*, **57**, 341.
- Carlson, J.M. & Langer, J.S., 1989. Mechanical model of an earthquake fault, *Phys. Rev. A*, **40**, 6470–6484.
- da Costa, F.P., Grinfeld, M. & Wattis, J.A.D., 2002. A hierarchical cluster system based on Horton-Strahler rules for river networks, *Studies Ap. Math.*, **109**, 163–204.
- Drossel, B. & Schwabl, F., 1992a. Self-organized critical forest-fire model, *Phys. Rev. Lett.*, **69**, 1629–1632.
- Drossel, B. & Schwabl, F., 1992b. Self-organized criticality in a forest-fire model, *Physica A*, **191**, 47–50.
- Fowler, A.D., 1990. Self-organized mineral textures of igneous rocks: the fractal approach, *Earth-Sci. Rev.*, **29**, 47–55.
- Gabrielov, A., Newman, W.I. & Turcotte, D.L., 1999. Exactly soluble hierarchical cluster model: inverse cascades, self-similarity and scaling, *Phys. Rev. E*, **60**, 5293–5300.
- Grassberger, P., 2002. Critical behaviour of the Drossel-Schwabl forest fire model, *New J. Phys.*, **4**, 17.
- Gutenberg, B. & Richter C.F., 1954. *Seismicity of the Earth and Associated Phenomenon*, 2nd edn, Princeton University Press, Princeton, New Jersey.
- Guzzetti, F., Malamud, B.D., Turcotte, D.L. & Reichenbach, P., 2002. Power-law correlations of landslide areas in central Italy, *Earth planet. Sci. Lett.*, **195**, 169–183.
- Horton, R.E., 1945. Erosional development of streams and their drainage basis: hydrophysical approach to quantitative morphology, *Geol. soc. Am. Bull.*, **56**, 275–370.
- Hovius, N., Stark, C.P. & Allen, P.A., 1997. Sediment flux from a mountain belt derived by landslide mapping, *Geology*, **25**, 231–234.
- Hovius, N., Stark, C.P., Hao-Tsu, C. & Jinn-Chuan, L., 2000. Supply and removal of sediment in a landslide-dominated mountain belt: Central Range, Taiwan, *J. Geol.*, **108**, 73–89.

- Malamud, B.D., Morein, G. & Turcotte, D.L., 1998. Forest fires: An example of self-organized critical behavior, *Science*, **281**, 1840–1842.
- Malamud, B.D., Turcotte, D.L., Guzzetti, F. & Reichenbach, P., 2004. Landslide inventories and their statistical properties, *Earth Surf. Process. Landforms*, **29**, 687–711.
- Mandelbrot, B., 1982. *The Fractal Geometry of Nature*, Freeman, San Francisco.
- Minnich, R.A. & Chou, Y.H., 1997. Wildland fire patch dynamics in the Chaparral of southern California and northern Baja California, *Int. J. Wildland Fire*, **7**, 221–248.
- Newman, W.I. & Turcotte, D.L., 2002. A simple model for the earthquake cycle combining self-organized complexity with critical point behavior, *Nonlinear Proc. Geophys.*, **9**, 453–461.
- Ossadnik, P., 1992. Branch order and ramification analysis of large diffusion limited aggregation clusters, *Phys. Rev. A*, **45**, 1058–1066.
- Peckham, S.D., 1995. New result for self-similar trees with application to river networks, *Water Resour. Res.*, **31**, 1023–1029.
- Pelletier, J.D., 1999. Self-organization and scaling relationships of evolving river networks, *J. geophys. Res.*, **104**, 7359–7375.
- Pelletier, J.D., Malamud, B.D., Blodgett, T. & Turcotte, D.L., 1997. Scale-invariance of soil moisture variability and its implications for the frequency-size distribution of landslides, *Eng. Geol.*, **48**, 255–268.
- Ricotta, C., Avena, G. & Marchetti, M., 1999. The flaming sandpile: self-organized criticality and wildfires, *Ecol. Mod.* **199**, 73–77.
- Rundle, J.B. & Jackson, D.D., 1977. Numerical simulation of earthquake sequences, *Seism. Soc. Am. Bull.*, **67**, 1363–1377.
- Rundle, J.B. & Klein, W., 1993. Scaling and critical phenomena in a cellular automaton slider-block model for earthquakes, *J. Stat. Phys.*, **72**, 405–412.
- Stauffer, D. & Aharony, A., 1994. *Introduction to percolation theory*, 2nd ed.
- Strahler, A.N., 1957. Quantitative analysis of watershed geomorphology, *Am. Geophys. Un. Trans.*, **38**, 913–920.
- Tokunaga, E., 1978. Consideration on the composition of drainage networks and their evolution, *Geographical Rep. Tokyo Metro. Univ.*, **13**, 1–27.
- Turcotte, D.L., 1997. *Fractals and Chaos in Geology and Geophysics*, 2nd edn, Cambridge University Press, Cambridge.
- Turcotte, D.L., 1999. Self-organized criticality, *Rep. Prog. Phys.*, **62**, 1377–1429.
- Turcotte, D.L., Malamud, B.D., Morein, G. & Newman, W.I., 1999. An inverse cascade model for self-organized critical behavior, *Physica A*, **268**, 629–643.
- Witten, T.A. & Sander, L.M., 1981. Diffusion-limited aggregation, a kinetic critical phenomenon, *Phys. Rev. Lett.*, **47**, 1400–1403.